



UMEÅ UNIVERSITET

The background of the cover is a photograph of a peat core cross-section. The core is stained with a color scale, likely representing the  $^{210}\text{Pb}$  concentration. The colors range from dark blue at the top to bright yellow and orange at the bottom, with various shades of green and cyan in between. The texture of the peat is visible, showing distinct layers and some root-like structures.

**The potential disturbance of the  $^{210}\text{Pb}$  profile in peat cores by roots and the implications for  $^{210}\text{Pb}$  dating.**

Nora Spjut

Supervisor: Carolina Olid

Examensarbete, 15 hp

Examensarbete i geovetenskap för kandidatexamen, 15 hp

Vt 2020



# **Nora Spjut**

## **Abstract**

At this moment there is a gap in information regarding the affect roots might have on  $^{210}\text{Pb}$  distribution in peat cores and in turn the obtained chronologies by  $^{210}\text{Pb}$  dating. Therefore, four peat cores were collected from the snow manipulation study site within the mire complex Storflaket (68°20048"N, 18°58016"E). Two cores from snow fence plots, which has experienced root growth due to permafrost thaw, and 2 cores from control plots.  $^{210}\text{Pb}$  distribution and the provided  $^{210}\text{Pb}$  chronologies were then compared with root content within and between the cores. In two of the cores (C5 and SF2) did subsurface peaks in the  $^{210}\text{Pb}$  activity profile follow the distribution profile of the dwarf shrub roots. The same pattern was not seen with Eriophorum roots. This indicates that presence of dwarf root with their shallow and horizontally growth can affect the  $^{210}\text{Pb}$  profile by horizontal translocation of  $^{210}\text{Pb}$ . The chronologies obtained by the CF:CS and CRS dating models could not be validated for the C5 core which suggest that dwarf shrub roots also can affect the  $^{210}\text{Pb}$  dating.

### **Key words**

Permafrost thaw

$^{210}\text{Pb}$  dating

Dwarf shrub roots



# Index

<b>1 Introduction</b> .....	1
<b>1.2 Aim</b> .....	2
<b>1.3 Questions to answer</b> .....	2
<b>2 Method</b> .....	2
<b>2.1 Study site</b> .....	2
<b>2.3 Lab analysis</b> .....	3
<b>2.4 <sup>210</sup>Pb dating methods</b> .....	3
<b>2.4.1 Constant initial concentration (CIC) model</b> .....	4
<b>2.4.2 Constant flux: constant sedimentation CF:CS model</b> .....	4
<b>2.4.3 Constant rate of supply (CRS) model</b> .....	4
<b>3 Results</b> .....	5
<b>3.1 Peat densities</b> .....	5
<b>3.1 Vertical distribution of radionuclides (<sup>210</sup>Pb, <sup>137</sup>Cs and <sup>7</sup>Be)</b> .....	6
<b>3.2 Roots distribution</b> .....	7
<b>3.4 Comparing roots and <sup>210</sup>Pb distributions</b> .....	8
<b>3.5 Dating models</b> .....	10
<b>4 Discussion</b> .....	11
<b>4.1 Distribution and accumulation of radionuclides in peat</b> .....	11
<b>4.2 Validation of <sup>210</sup>Pb dating models</b> .....	11
<b>4.3 Processes that affect the dating of the peat cores</b> .....	12
<b>References</b> .....	13



# 1 Introduction

Peat bogs are commonly used as archives for studying past environmental conditions. For example, pollen found along collected peat cores can be used to examine vegetation changes in the landscape through the years (Ralska-Jasiewiczowa et al 2006).

Furthermore, macrofossils and analysis of peat humification can be used to study climate changes (Castro et al 2014). Peat cores also contain relevant information about past atmospheric deposition of metal pollutants (Marx et al 2009) and (Pratte et al 2013) and other airborne pollutants like mercury (Hg) (Drexler et al. 2016). Peat bogs have also been widely studied because of their role in the global carbon cycle (Dorrepaal et al 2009). To be able to use these records as archives, we need to establish methods that can give accurate chronologies for the peat cores.

Radiometric techniques are commonly used in geochronology and applied when dating peat records. The radionuclide  $^{14}\text{C}$  ( $T_{1/2} = 5730$  years) can be used to date organic materials and date individual layers in the peat record. This method allows to establish chronologie for the whole Holocene and the latest part of the Pleistocene (Gong et al 2017, Haesaerts et al 2010). However, inaccuracies in the derived dates can be obtained when material in the analysed layer such as roots is not correctly sorted during sampling, leading to younger ages for these layers where roots have penetrated (Ralska-Jasiewiczowa et. al 2006). The natural radionuclide  $^{210}\text{Pb}$  ( $T_{1/2} = 22,3$  years) is used as a dating method for sedimentary deposits that has accumulated during the past 100-150 years. The method has been proven to work well for lake sediments (Appleby 2001) and has during the past decades also been applied in the dating of peat cores. One advantage with the  $^{210}\text{Pb}$  dating is that the method provides a continuous chronology for the record for the past century (Appleby et al 1997 and Olid et al 2010). The artificial radionuclide  $^{137}\text{Cs}$  is used as an individual dating marker to validate the  $^{210}\text{Pb}$  chronology (Olidfield et al 1995, Bao et al 2010 and Davies et al 2018).  $^{137}\text{Cs}$  was dispersed into the environment during the nuclear weapon testing period, with maximum emissions occurring in 1963 (UNSCEAR 2000). More recently, the Chernobyl accident in 1986 released significant quantities of  $^{137}\text{Cs}$  into the northern hemisphere with deposition mostly occurring in Europe. In undisturbed archives, these events have resulted in well-defined peaks along the peat record and can therefore be used to identify the 1963 and 1986 layers (Appleby 2001). It has been noted, however, that the retention of the  $^{137}\text{Cs}$  record depend on the mineral content, having a higher retention in minerogenic mires (MacKenzie et. al 1997).

One of the main assumptions in the most common  $^{210}\text{Pb}$  dating models is that  $^{210}\text{Pb}$  is immobilised in peat. The chronologies from these models is therefore obtained from the accumulation of atmospheric deposited  $^{210}\text{Pb}$  what is bound to the organic matter and retained in the peat (Vile et al 1999). The retention of atmospheric deposited  $^{210}\text{Pb}$  has in some studies been proven by comparing the measured  $^{210}\text{Pb}$  atmospheric flux from peat cores with previously noted fluxes from the same region (Bao et al. 2010, Appleby et al. 1997 and Mackenzie et al 1997). Some limitations in the  $^{210}\text{Pb}$  dating method has however been observed when these models have been applied in peat cores. In part due to that a peat bog is quite heterogeneous regarding vegetation, surface morphology and humification and all this results in a varying deposition rate of atmospheric elements within the peat bog. Which in turn results in variations in the total element inventories (Bindler et al 2004). Surface vegetation has also been proven to have a strong influence on the  $^{210}\text{Pb}$  dating. Olid et al. 2008 showed that  $^{210}\text{Pb}$  inventories could be underestimated with 39-49% if the surficial vegetation layer were not included in the dating models The retention of  $^{210}\text{Pb}$  in peat has been noted to be lower in the uppermost layers of the peat core. This section is often not highly decomposed, which indicate that lower peat densities promote  $^{210}\text{Pb}$  mobility (Biester et al 2007). This hypothesis has been confirmed using laboratory experiments, were the retention of deposited  $^{210}\text{Pb}$  at the peat surface layer (0-2 cm) was shown to vary between 21-85 % and was strongly depending on precipitation intensity (Hanon et al 2015). To examine the potential downwash of  $^{210}\text{Pb}$  in peat, some studies has looked at the distribution of  $^7\text{Be}$  ( $T_{1/2} = 54$  days) distribution in

the peat profiles (Hansson et al 2014, Taylor et al 2012). Due to the short half-life of  $^7\text{Be}$ , dose a detection of  $^7\text{Be}$  below the surface layer mean that some percolation has occurred in the peat profile. The retention of  $^{210}\text{Pb}$  in the upper parts of the peat core is often lesser than at depth indicating that the correlating lower peat densities promote  $^{210}\text{Pb}$  mobility (Biester et al. 2007).

Previous studies have as mentioned above examined the implication on the  $^{210}\text{Pb}$  dating for properties such as density and plant community. However, there is a gap in information regarding which role roots has on the  $^{210}\text{Pb}$  dating. As a response to global warming and the thawing of permafrost plant communities in peat bogs from the northern region have experienced a shift in vegetation from Sphagnum to predominantly vascular plants (Johansson et al 2013 and Blume- Werry et al 2018). This shift will lead to variations in peat accumulation rate because of the direct link to which sort of plants that are present and to the formation of a lower density peat at the surface compared to Sphagnum- dominated mires. (Malmer and Wallén 1999). The question is however these new roots may act as channels and facilitate vertical translocation of atmospheric deposited elements on the surface to deeper layers, which in turn would affect the  $^{210}\text{Pb}$  chronology.

In this study we examine the distribution of  $^{210}\text{Pb}$  in cores collected from a snow manipulation study site. In which higher snow accumulation in snow fence plots has led to a new dominantly vascular plant community compared to control plots. By comparing  $^{210}\text{Pb}$  profiles and their derived chronologies with the root distribution in the cores, the potential impact of roots on establishing accurate chronologies from  $^{210}\text{Pb}$  dating is evaluated.

## 1.2 Aim

Examine if the presence of roots affects the distribution of  $^{210}\text{Pb}$  in peat and it's repercussions on the  $^{210}\text{Pb}$  chronologies.

## 1.3 Questions to answer

1. Is the  $^{210}\text{Pb}$  record affected when vegetation with long roots develop?
2. How does this affect the  $^{210}\text{Pb}$  chronology?
3. Does this process affects similarly the distribution of other radionuclides used for dating ( $^{137}\text{Cs}$ ).

# 2 Method

## 2.1 Study site

The study site is located on a peat plateau within the mire complex Storflaket (68°20048"N, 18°58016"E) in northernmost Sweden, 6 km east of the Abisko Scientific Research station. The plateau contains permafrost and has been the location for a snow manipulation experiment since 2005. In the experiment six randomly selected plots ("manipulated plots") were selected to erect snow fences (10 m long, 1 m tall) during the winter months (September to late May/ early June) to trap snow and promote permafrost thawing. Six other randomly selected plots without treatment (controls) were selected as references. Increased snow cover resulted in an increased mean winter ground temperature by 1,85 and 1,4 °C at 15 and 30 cm depth, respectively. The higher ground temperature in turn increased active layer thickness to 98 cm in manipulated plots compared to 62 cm in control plots. The thawing of permafrost in manipulated plots induced surface subsidence of 24 cm, while only 5 cm surface subsidence was observed in the control plots between 2005 and 2012. The more visible effect of the Treatment was the changes that occurred in surface vegetation, with a shift from *Sphagnum* to more vascular plants, predominantly *Eriophorum vaginatum* (Johansson et al. 2013). Root distribution and growth were also affected, observing that dwarf shrub roots stayed in the



upper part of the active permafrost layer while *Eriophorum* roots followed the thaw front and led to root growth in previously well protected peat (Blume- Werry et al 2019). The snow manipulation experiment and the resulting shift in surface vegetation and root growth enhancement provides an excellent setup for studying the implication of the presence of root on the  $^{210}\text{Pb}$  distribution in peat. This study was performed using two cores collected from snow fence plots (SF2 and SF3) and two cores collected from control plots (C2 and C5).

### 2.3 Lab analysis

Each one of the four cores were divided into two halves. One of the halves was sent out for root analysis to obtain information about the root content and type of roots along the profile. Root content and type were determined for every two centimetres. The area of each sections was measured to allow for root density calculations. All sections were dried at 70 °C for 72h and the dry weight of the different types of roots was measured.

The second halves of the cores were kept for dating purposes. The upper living vegetation was collected as one section following Olid et al. 2008. All cores were sliced into 2 cm sections in the upper part of the cores (2-8 cm interval), where the plants were not completely decomposed, and individual plants were still distinguishable. Below this part, all cores were sliced into 1 cm sections. Sections were cut into well-defined squares to allow for accurate density estimations. All samples were placed into weighted plastic bags and dried at 65°C. The dry samples were then weighed, and dry peat density calculated. Part of the samples were prepared for  $^{210}\text{Pb}$  analysis using alpha spectrometry. This analysis was done following an acid digestion method described in Sanchez- Cabeza et al 1997. The method determines the  $^{210}\text{Pb}$  activity by measuring the activity of its daughter nuclide  $^{210}\text{Po}$ , which is assumed to be in secular equilibrium. Po sources were measured using Ortec ULTRA-AS Ion-Implanted-Silicon Charged- Particle Detectors (Model U-020-450-AS). To validate the  $^{210}\text{Pb}$ -derived chronology, samples were also analysed using gamma spectrometry to determine the distribution of  $^{137}\text{Cs}$  and  $^7\text{Be}$ . Gamma spectrometry was performed using a high-purity intrinsic Ge detector (CANBERRA, model GCW3523).

### 2.4 $^{210}\text{Pb}$ dating methods

The  $^{210}\text{Pb}$  radionuclide is part of the  $^{238}\text{U}$  decay series (figure 1).  $^{210}\text{Pb}$  activity found sedimentary deposits like lake sediments and peat cores can be divided into two different compartments. One, the unsupported  $^{210}\text{Pb}$  activity that derives from atmospheric deposition of  $^{210}\text{Pb}$ . This fraction is produced in the atmosphere by the decay of  $^{222}\text{Rn}$  that escapes from soils during the decay of  $^{226}\text{Ra}$ . Two, the supported fraction of  $^{210}\text{Pb}$  in turn derives from in situ decay of the parent nuclide  $^{226}\text{Ra}$ . The unsupported  $^{210}\text{Pb}$  fraction can be calculated by subtracting the supported  $^{210}\text{Pb}$  activity from the total  $^{210}\text{Pb}$  activity. In this study, the supported  $^{210}\text{Pb}$  activity was estimated from the average value of the  $^{210}\text{Pb}$  activity in the bottom sections of the cores.

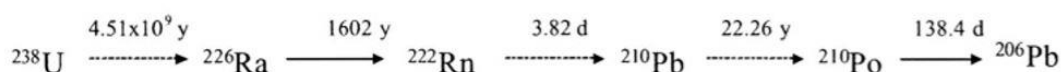


**Figure 1.** The decay series for  $^{238}\text{U}$  and the half-life of respective radionuclide.

The three most used  $^{210}\text{Pb}$  dating models use the distribution of unsupported  $^{210}\text{Pb}$  to obtain chronologies for sedimentary deposits accumulated over the past 100-150 years (Appleby 2001). All these models assume that  $^{210}\text{Pb}$  is retained in the record and a constant atmospheric flux of  $^{210}\text{Pb}$ .

#### **2.4.1 Constant initial concentration (CIC) model**

The CIC dating model assumes that the initial concentration of  $^{210}\text{Pb}$  in the surface layer is constant even if changes occur in the rate of peat accumulation. The method uses equation 1 to obtain the chronologies for the cores (Appleby 2001).

$$\text{Eq. 1 } t = 1/\lambda * \ln(C(o)/C(x))$$

Where  $\lambda$  is the radioactive decay constant (0,0311  $\text{y}^{-1}$ ),  $C(o)$  is the  $^{210}\text{Pb}$  activity ( $\text{Bq kg}^{-1}$ ) at the surface of the core and  $C(x)$  is the  $^{210}\text{Pb}$  activity ( $\text{Bq kg}^{-1}$ ) at certain depth  $x$ . Organic matter decay causes the initial  $^{210}\text{Pb}$  activities at the surface to change, making the CIC model inappropriate to date peat records because a constant initial activity of  $^{210}\text{Pb}$  cannot be assumed (Olid et al., 2008) therefore have the method not been used in this study.

#### **2.4.2 Constant flux: constant sedimentation CF:CS model**

The CF:CS dating model assumes a constant rate of peat accumulation. The mean peat accumulation rate can be inferred from the mean slope of the regression line obtained by plotting the unsupported  $^{210}\text{Pb}$  activity against the cumulative mass. The method uses equation 2 to obtain the chronologies for the cores.

$$\text{Eq. 2 } t = m/r$$

Where  $m$  is the cumulative mass ( $\text{g cm}^{-2}$ ) from the top of the core to the certain depth  $x$  and  $r$  is the mean accumulation rate ( $\text{g cm}^{-2} \text{yr}^{-1}$ ) (Appleby 2001).

#### **2.4.3 Constant rate of supply (CRS) model**

The CRS model assumes a constant deposition rate of unsupported  $^{210}\text{Pb}$  from the atmosphere. The method uses equation 3 to obtain the chronologies for the cores.

$$\text{Eq. 3 } t = 1/\lambda * \ln(A(o)/A(x))$$

Where  $\lambda$  is the  $^{210}\text{Pb}$  radioactive decay constant (0,0311),  $A(o)$  is the total unsupported  $^{210}\text{Pb}$  inventory and  $A(x)$  is the unsupported  $^{210}\text{Pb}$  inventory from the depth of limit of detection of atmospheric deposited  $^{210}\text{Pb}$  in the core to the depth  $x$  (Appleby 2001).

The uncertainties for the dating methods were calculated using the quadratic law of propagation including uncertainties from the analyses mass weight, tracer volume added, and the counting errors obtained in the alpha spectrometry.

### 3 Results

#### 3.1 Peat densities

Peat density profiles for all cores are shown in figure 2. Cores C5, SF2 and SF3 showed a general trend of increasing density with depth. C5 showed a slight increase in peat density at 15 cm depth. C2 in turn showed a decrease in peat density in the upper 5 cm. Also, the surface density in C2 of  $0,176 \text{ g cm}^{-3}$  was around 2 times higher when those for the rest of the cores. The greatest density changes occurred for SF2, where density drastically increased between 15 and 25 cm depth, from  $0,2 \text{ g cm}^{-3}$  to around  $1 \text{ g cm}^{-3}$ .

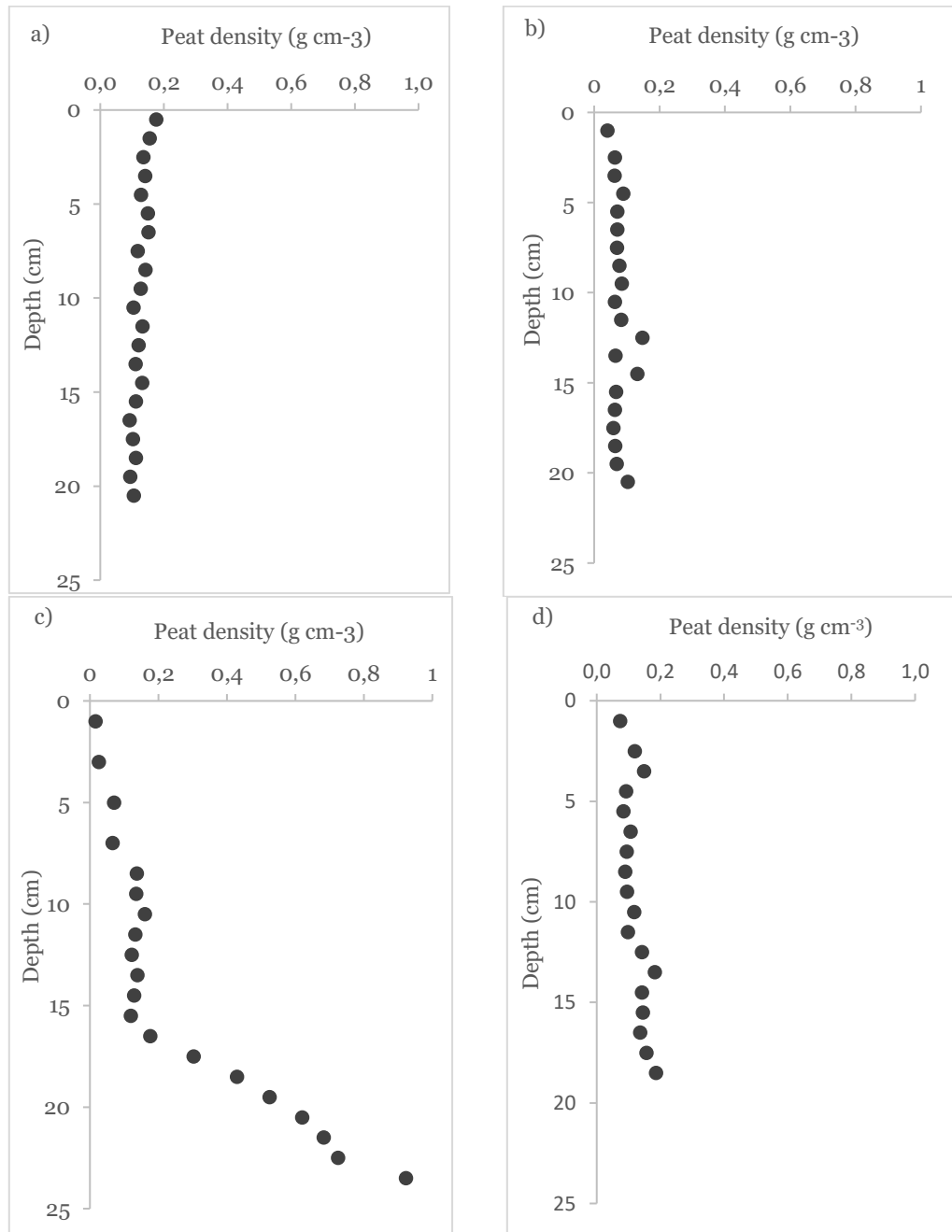


**Figure 2.** Peat density profiles for a) C2 b) C5 d) SF2 and SF3.

### 3.1 Vertical distribution of radionuclides ( $^{210}\text{Pb}$ , $^{137}\text{Cs}$ and $^7\text{Be}$ )

The vertical distribution of  $^{210}\text{Pb}$ ,  $^{137}\text{Cs}$  and  $^7\text{Be}$  are shown in figure 3. For C5, SF2 and SF3 was unsupported  $^{210}\text{Pb}$  detected up to 14-17 cm depth. C2, however showed measurable activities of unsupported  $^{210}\text{Pb}$  only in the upper 5 cm. Only C2 and Sf3 showed clearly the expected exponential decay of unsupported  $^{210}\text{Pb}$  with depth. Small deviations from this trend were, however, observed in the upper 5 cm of SF3. Significant deviations from the exponential decay profile were observed in the C5. For this core, the activities of  $^{210}\text{Pb}$  did not follow a clear pattern in the upper 5 cm and an extremely high peak in  $^{210}\text{Pb}$  activity ( $132 \text{ Bq kg}^{-1}$ ) was located at 15 cm depth). Core SF2 stood out from the other cores, having a subsurface peak in unsupported  $^{210}\text{Pb}$  at 8,5 cm depth. SF2 also showed two times lower unsupported  $^{210}\text{Pb}$  activities in the upper layers then the rest of the cores.

$^{137}\text{Cs}$  activity were detected in all cores up to a depth of 14- 15 cm. Control plots showed maxima in  $^{137}\text{Cs}$  activity in the upper layers (0.5- 1 cm) with values ranging from 60 to 100  $\text{Bq kg}^{-1}$ . In snow fence plots, however,  $^{137}\text{Cs}$  activity did not exceed  $32 \text{ Bq kg}^{-1}$  through the profiles. In C2 a secondary  $^{137}\text{Cs}$  peak ( $19 \text{ Bq kg}^{-1}$ ) were observed at 4 cm depth. Bellow 6 cm depth in C2,  $^{137}\text{Cs}$  activities kept to an almost constant activity around  $7\text{-}8 \text{ Bq kg}^{-1}$ . For C5, SF2 and SF3 subsurface maxima of  $^{137}\text{Cs}$  were observed in the depth intervals 4.5 to 5.5 cm and 8.5 to 9.5 cm.

Activities of  $^7\text{Be}$  were found in the upper 5 cm of C2, with a profile that followed an exponential curve. Some  $^7\text{Be}$  was also detected in the two upper layers of SF3.

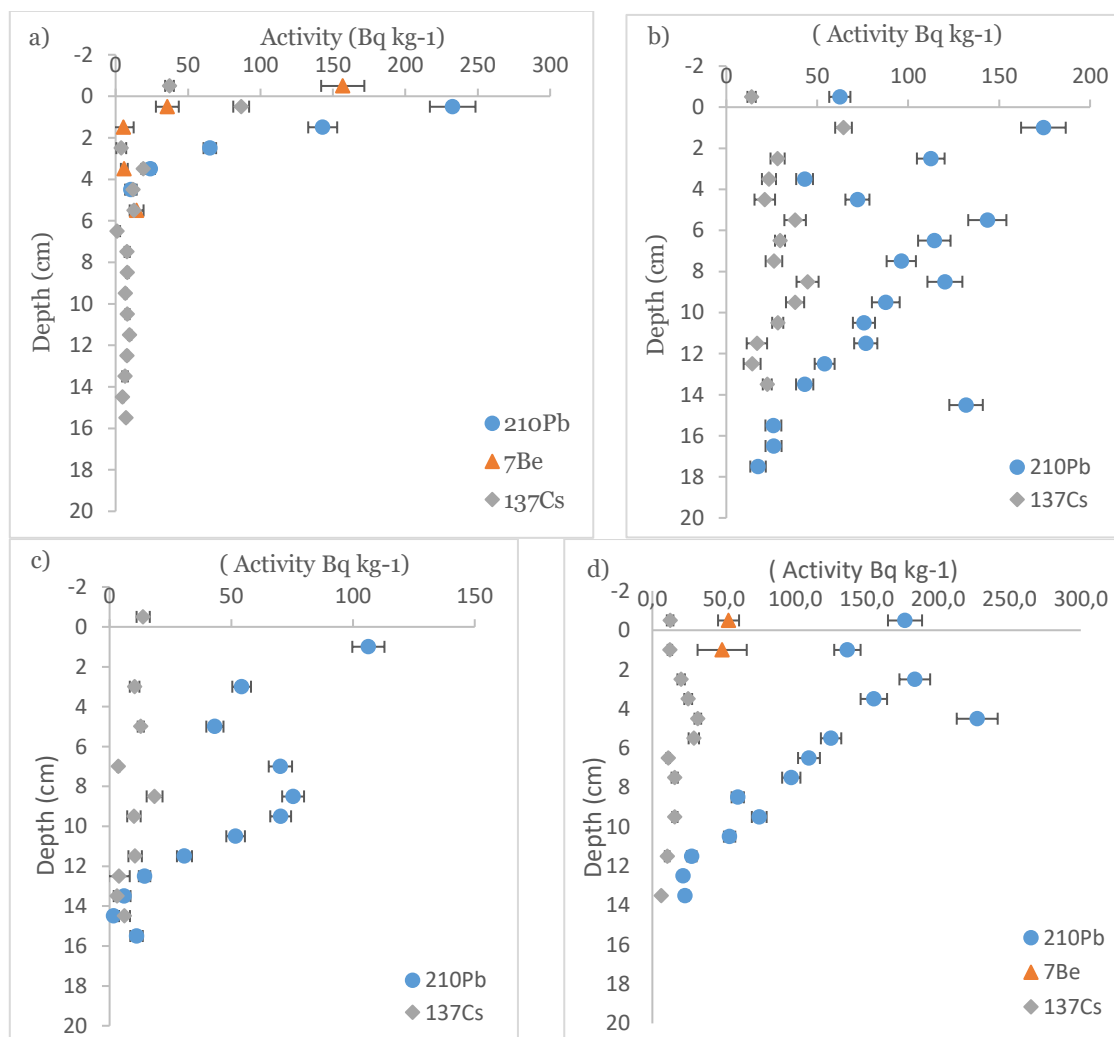


**Figure 3.** Unsupported  $^{210}\text{Pb}$ ,  $^7\text{Be}$  and  $^{137}\text{Cs}$  activity in  $\text{Bq kg}^{-1}$  for a) C2 b) C5 c) SF2 and d) SF3.

Total unsupported  $^{210}\text{Pb}$  and  $^{137}\text{Cs}$  inventories were calculated from their profiles in all of the cores (Table 1). Core SF2 had the lowest  $^{210}\text{Pb}$  inventory with  $583 \pm 16 \text{ Bq m}^{-2}$ . SF2 had also the lowest  $^{137}\text{Cs}$  inventory with  $98 \pm 16 \text{ Bq m}^{-2}$ . The highest  $^{210}\text{Pb}$  inventory was found in the SF3 core with  $1748 \pm 36 \text{ Bq m}^{-2}$ . The highest  $^{137}\text{Cs}$  inventory were however found in C2 and C5 with around  $300 \text{ Bq m}^{-2}$ .

**Table 1.**  $^{210}\text{Pb}$  Atmospheric flux ( $\text{Bq m}^{-2} \text{ yr}^{-1}$ ), total  $^{210}\text{Pb}$  inventory ( $\text{Bq m}^{-2}$ ) and total  $^{137}\text{Cs}$  inventory for the cores.

Core	C2	C5	SF2	SF3
$^{210}\text{Pb}$ atmospheric flux ( $\text{Bq m}^{-2} \text{ yr}^{-1}$ )	$23 \pm 1$	$36 \pm 0.7$	$18 \pm 0.5$	$54 \pm 1.1$
Unsupported $^{210}\text{Pb}$ inventory ( $\text{Bq m}^{-2}$ )	$769 \pm 33$	$1163 \pm 25$	$583 \pm 16$	$1748 \pm 36$
$^{137}\text{Cs}$ inventory ( $\text{Bq m}^{-2}$ )	$303 \pm 12$	$304 \pm 14$	$98 \pm 10$	$217 \pm 8$

### 3.2 Roots distribution

Root distribution for all cores is shown in figure 4. Dwarf shrub and *Eriophorum* roots followed for the most part a similar distribution within the separate cores. The main root distribution, however, differed between the control plots and the manipulated plots. As expected, were the root density greater in the snow fence plots. This was however, mostly explained by the observed increase of *Eriophorum* roots. While SF2 showed *Eriophorum* root densities of  $20 \text{ mg cm}^{-3}$ , were the same observed densities 4 times lower in C2, C5 and SF3. For SF3, dwarf shrub and *Eriophorum* root densities did not exceed those found in the control plots. The difference instead being that SF3 had almost constant densities of dwarf shrub and *Eriophorum* roots around  $2\text{-}4 \text{ mg cm}^{-3}$  through the whole peat profile. In snow fence plots were root content low in the surface layer and most of the roots were distributed bellow 5 cm. In contrast, control plots showed distinct peaks of dwarf shrub roots in the upper layers and an overall lower root content at depth. C2, however did also have a clear increase of dwarf shrub roots and *Eriophorum* roots at a 20 cm depth

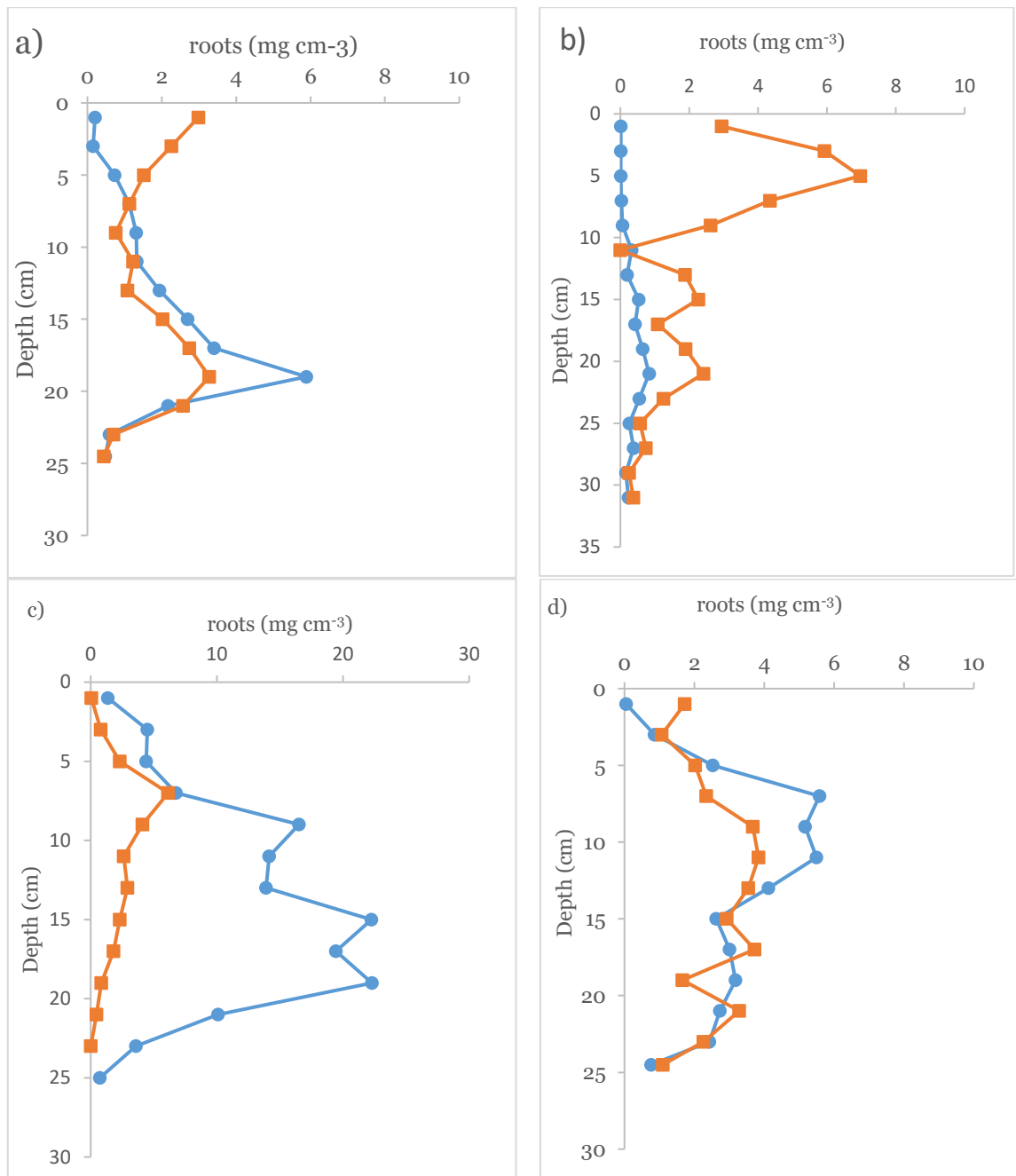


**Figure 4.** Root content in  $\text{g cm}^{-3}$  for Eriophorum roots (blue line with circles) and Dwarf shrub roots (orange line with squares) for a) C2 b) C5 c) SF2 and d) SF3.

### 3.4 Comparing roots and $^{210}\text{Pb}$ distributions

$^{210}\text{Pb}$  activities for every two centimetres in the cores were re-calculated in order to compare with the root density (figure 5). Correlation between dwarf shrub roots and  $^{210}\text{Pb}$  activities could be observed in C5 were they followed the same trend between 9 and 17 cm depth. In SF2, a similar trend was observed around the 8 cm depth.

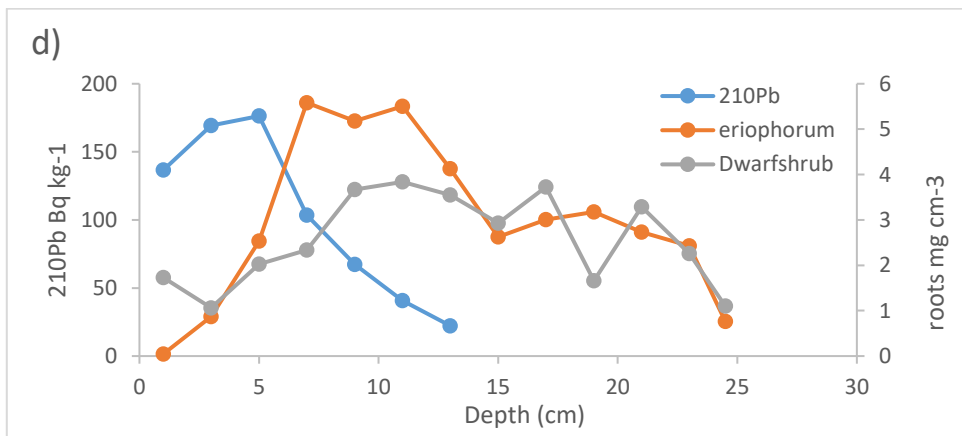
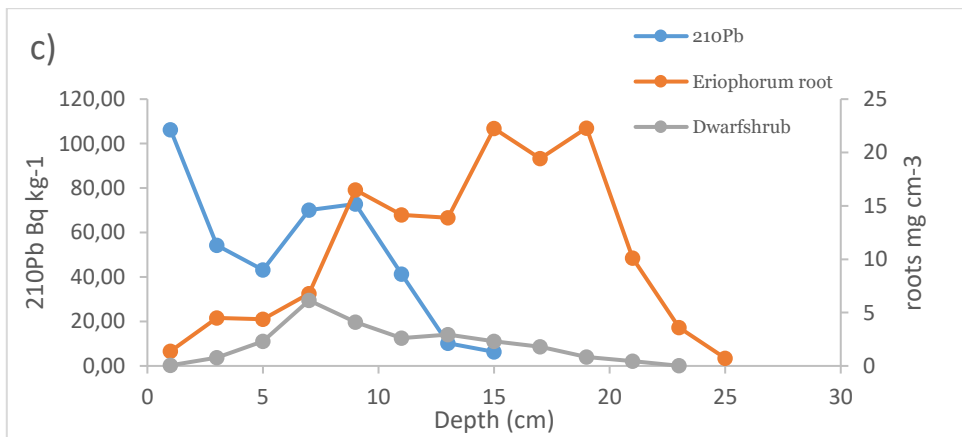
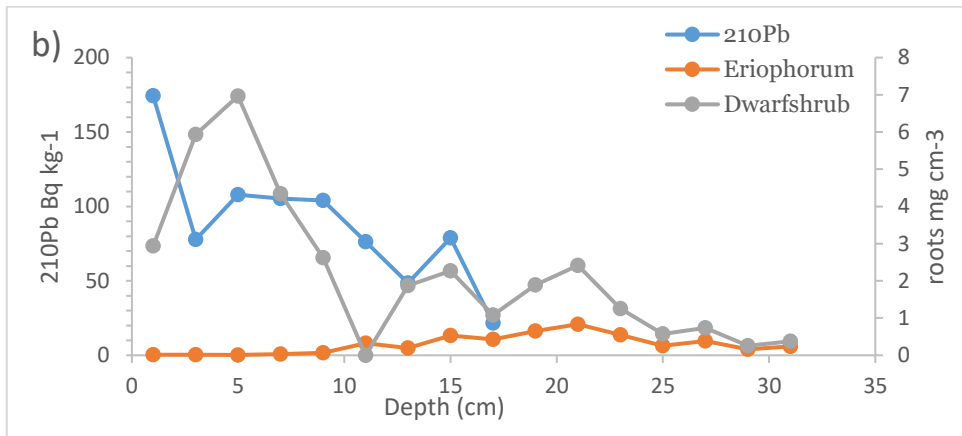
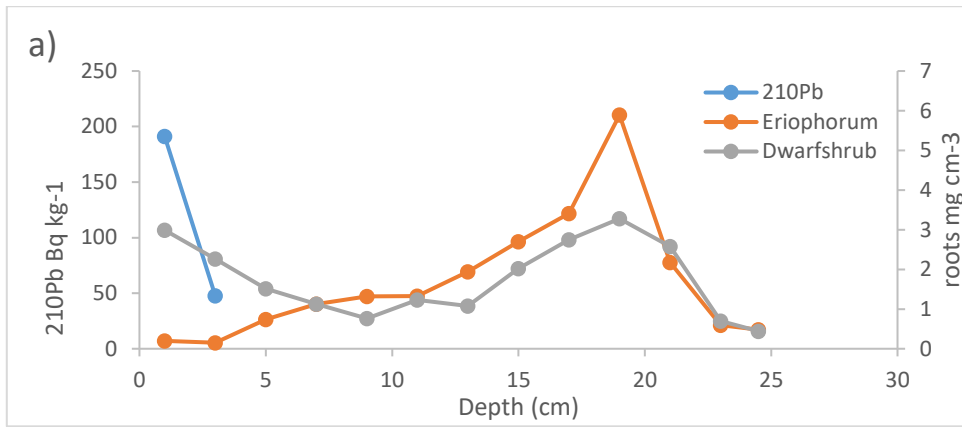


**Figure 5.** <sup>210</sup>Pb activities and root densities for every 2 cm of the peat cores a) C2 b) C5 c) SF2 and d) SF3.

### 3.5 Dating models

The results of the dating of the four cores are shown in figure 6. For C2, the CRS and SF:CS models did not provide consistent chronologies with the  $^{137}\text{Cs}$  record for the upper part of the core. The CF:CS model did however provide an accurate chronology for the 1963 depth. For C5 neither the CF:CS nor the CRS model provided reliable chronologies when comparing to dates obtained from peaks of  $^{137}\text{Cs}$ . For SF2 did the CF:CS dating model provided the most consistent chronology for the core when compared with the peaks in the  $^{137}\text{Cs}$  profile. However, the uncertainties associated to this chronology were quite high, up to 30 years for the same layer. The CRS model gave a consistent chronology for the SF3 core, with ages in agreement with those provided by  $^{137}\text{Cs}$ .

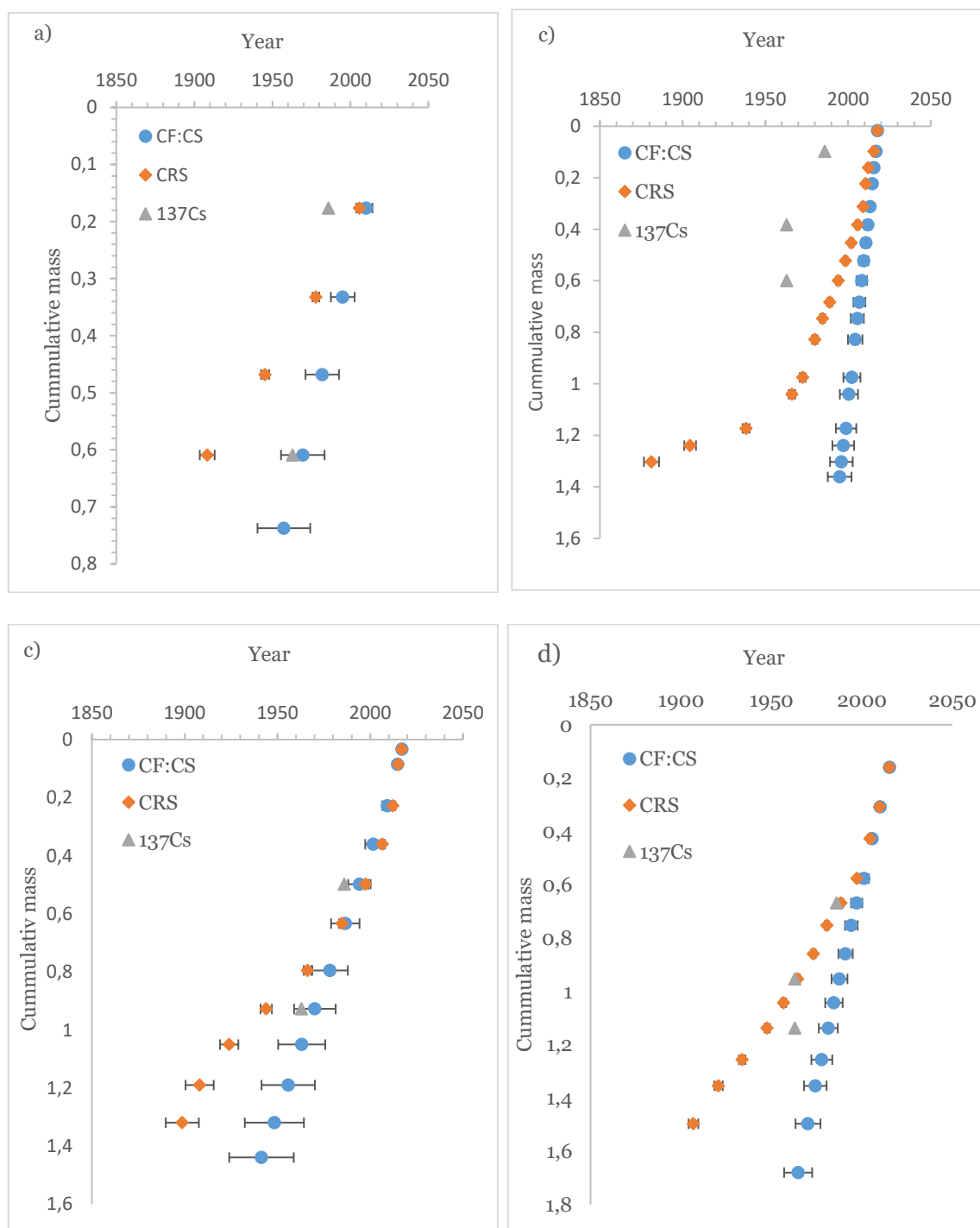


**Figure 6.** Chronologies from the CF:CS and CRS dating models for a) C2 b) C5 c) SF2 and d) SF3, plotted against cumulative mass and compared to dates obtained from the  $^{137}\text{Cs}$  profile.



## 4 Discussion

### 4.1 Distribution and accumulation of radionuclides in peat

The use of  $^{210}\text{Pb}$  to obtain chronologies for the past 100- 150 years was originally developed for dating closed systems like lake sediments (Appleby 2001). In these closed systems the  $^{210}\text{Pb}$  profile most often show the expected exponential decay profile and the dating methods works well (MacKenzie et al 2010 and Zalewska et al. 2020) Peat bogs, however, are a more open system and the accumulation and retention of  $^{210}\text{Pb}$  can be affected by multiple processes. This is reflected in the results from this study.

The distribution of  $^{210}\text{Pb}$  activities in C5 and SF3 showed deviation from the expected exponential decay profile in the uppermost layers that correlated with low peat density. This trend has been remarked upon in previous studies that has examined the accumulation of atmospheric deposited elements in the upper acrotelm and suggests that post depositional processes such as smearing may have affected the  $^{210}\text{Pb}$  record in this upper compartment (Biester et al 2007). C5 and SF2 cores did show deviation from the expected exponential decay profile at depth. The unexpected high subsurface  $^{210}\text{Pb}$  activities at 15 cm depth in C5 and around 8,5 cm depth in SF2 are coincident with high peat density. This is especially notable in core C5 where peat density shows a peak around 15 cm depth. Suggest higher  $^{210}\text{Pb}$  accumulation due to increases in peat accumulation rate at these depths, it can also be consistent with our hypothesis that some  $^{210}\text{Pb}$  could have migrated from the upper layers and been accumulated at depth, where the higher compaction of the record restricts its vertical transport.

Unsupported  $^{210}\text{Pb}$  inventories from the control plots returned atmospheric  $^{210}\text{Pb}$  fluxes from 23 to 36  $\text{m}^{-2} \text{yr}^{-1}$ , while they in snow fence plots ranged between 18 to 54  $\text{m}^{-2} \text{yr}^{-1}$ . These values are comparable with ranges found in 12 other cores from the same mire of 12 to 31  $\text{Bq m}^{-2} \text{yr}^{-1}$  (Olid. Personal communication) and with measured fluxes of 19-38  $\text{Bq m}^{-2} \text{yr}^{-1}$  in northern Finland (Paatero et al 2015). However, the three times higher inventory in SF3 compared to SF2 and the two times higher inventory in SF3 compared to C2 indicate that multiple processes might have affected the  $^{210}\text{Pb}$  distribution in our studied cores. The lower total  $^{210}\text{Pb}$  inventories in C2 and SF2 may indicate that some fractions of  $^{210}\text{Pb}$  has been lost from these records. The SF3 core seems to have the most intact  $^{210}\text{Pb}$  record due to its higher  $^{210}\text{Pb}$  inventory and, if compared to the results from C5, it could be argued that C5 have had some losses of  $^{210}\text{Pb}$  too.

When looking at the total  $^{137}\text{Cs}$  inventories, control cores had inventories of around 300  $\text{Bq m}^{-2}$ , being around three times higher than  $^{137}\text{Cs}$  inventories found in SF2. The different between- core variability observed for  $^{210}\text{Pb}$  and  $^{137}\text{Cs}$  inventories suggest differential movement and retention of  $^{210}\text{Pb}$  and  $^{137}\text{Cs}$  in the cores. This agrees with previous studies that have shown that  $^{137}\text{Cs}$  can be mobile in peat while the  $^{210}\text{Pb}$  record is intact (Mackenzie et al. 1997).

### 4.2 Validation of $^{210}\text{Pb}$ dating models

To validate the chronologies obtained from the CF:CS and CRS dating models, we used  $^{137}\text{Cs}$  as an independent dating marker. Although some earlier studies have proven that  $^{137}\text{Cs}$  is highly mobile in peat (Mackenzie et al. 1997), some other studies have proven that the shape of the  $^{137}\text{Cs}$  profile is sometimes maintained and peaks in activity can still work as indicators of 1963 and 1986 year levels in peat (Olid et al 2008 and Bao et al 2010). For C2, the CF:CS model accurately provided the year  $1969 \pm 14$  for the subsurface peak in  $^{137}\text{Cs}$  that located the 1996 depth layer. However, the consistency seen at depth is not observed then comparing these dating methods in the upper part of the core, where the 1986 year fails to be located by both the CF:CS and CRS model (figure 5). This result together with the lower  $^{210}\text{Pb}$  inventory compared to the rest of the cores and with the presence of  $^7\text{Be}$  in the upper 5 cm indicate that  $^{210}\text{Pb}$  has been vertically translocated in upper part of the core. Due to this affect location in the upper layers are the deeper ages not affected (Olid et al. 2013) and wherefore can the 1963 peak be identified.

Core C5 showed clear deviations from the expected exponential decay profile for  $^{210}\text{Pb}$  for the upper 10 cm and this led to inconsistencies between  $^{137}\text{Cs}$  and  $^{210}\text{Pb}$  dating for both the CF:CS and CRS model. This indicates that the alterations of the  $^{210}\text{Pb}$  record have not been caused by changes in the accumulation rate but, most likely, by post depositional processes. This conclusion is strengthened by the fact that in this core both  $^{137}\text{Cs}$  and  $^{210}\text{Pb}$  follow the same pattern with depth, which contradict their differential depositional histories (UNSCEAR, 2000 and Beks et al. 1998).

Similar to C5, SF2 also showed deviations in the  $^{210}\text{Pb}$  profile. The CF:CS dating model returned the dates  $1994\pm 6$  and  $1970\pm 7$  for the  $^{137}\text{Cs}$  peaks of 1986 and 1963, respectively. Which is a bit older than expected but not much. However, the CF:CS model locate the ages  $1987\pm 8$  and  $1963\pm 7$  in the layers just below the observed  $^{137}\text{Cs}$  peaks, which raises the question if the  $^{210}\text{Pb}$  profile has been dislocated downward in the peat core. This in combination with the up to three times lower  $^{210}\text{Pb}$  inventory compared to the rest of the cores would indicate some  $^{210}\text{Pb}$  mobility.

Finally, for SF3 the  $^{137}\text{Cs}$  record seemed to validate the chronology obtained by the CRS model even if some smearing of the  $^{137}\text{Cs}$  profile has occurred at the 1963 depth in the core. This model assigned the dates  $1989\pm 1$  and  $1965\pm 1$ , for the  $^{137}\text{Cs}$  peak in 1998 and  $^{137}\text{Cs}$ , respectively.

#### **4.3 Processes that affect the dating of the peat cores**

Even if the cores that had alterations to the  $^{210}\text{Pb}$  profiles were identified by similar characteristics (low inventories, deviations from the expected exponential decay profile, and younger ages obtained at the surface by the  $^{210}\text{Pb}$  dating), the processes that has caused these discrepancies might be different.

For C2, the low  $^{210}\text{Pb}$  inventory and the inconsistency in the  $^{210}\text{Pb}$ - ages for the upper part of the core is likely due to the vertical mobility of  $^{210}\text{Pb}$  in peat. This is confirmed by the presence of the naturally occurring tracer  $^7\text{Be}$  (Tylor et al. 2011 and Hansson et al 2014) to a depth of 5 cm in the core.

SF2 and C5 showed significant disturbances in the  $^{210}\text{Pb}$  profiles. However,  $^7\text{Be}$  was not detected in these cores indicating that no vertical smearing of  $^{210}\text{Pb}$  has occurred after deposition. When the  $^{210}\text{Pb}$  profiles for C2 and C5 were compared to the root density distribution, significant correlations were observed between dwarf shrub roots and  $^{210}\text{Pb}$  disturbances (figure 4). Dwarf shrub roots are shallow roots and expand horizontally under growth, a pattern that has been shown to continue even if permafrost thaws and where is a thicker active layer available for the roots to grow in (Wang et al. 2016 and Blume-Werry et al 2019). These results would indicate that dwarf shrubs can cause a horizontally migration of  $^{210}\text{Pb}$  and therefore both be able to facilitate decreases and increases in the  $^{210}\text{Pb}$  profiles depending on in which direction the roots grow. The  $^{137}\text{Cs}$  profile followed the same pattern as the  $^{210}\text{Pb}$  profile in the upper 12 cm of C2 and C5. It seems wherefore likely that  $^{137}\text{Cs}$  is affected by the same horizontally migration and indicates that roots can affected this artificial radionuclide. No trend was observed when Eriophorum roots were compared to the  $^{210}\text{Pb}$  profile indicating that vertical root growth does not affect the  $^{210}\text{Pb}$  distribution.

Also mentionable is that induced surface subsidence in the snow fence plots could be responsible for inconsistency in the  $^{210}\text{Pb}$  profile. This process could therefore have affected the dating of the SF2 and SF3. However, both snow fence plots do not show losses in  $^{210}\text{Pb}$  which would suggest that this process do not affect the  $^{210}\text{Pb}$  record in these plots to a greater extent. It could however explain some of the loss in the inventory of the more mobile  $^{137}\text{Cs}$  in the snow fence cores compared to the control plots.

## References

- Appleby, P,G, Shotyk, W, Fankhauser, A. (1997) Lead- 210 ae dating of three peat cores in the jura mountains, Switzerland. *Water, air and soil pollution* (100) p. 223-231
- Bao,K, Xia,W, Lu, X and Wang, G. 2010. Recent atmospheric lead deposition recorded in an ombotrophic peat bog of Great Hinggan Mountains, Northeast China, from <sup>210</sup>Pb and <sup>137</sup>Cs dating. *Journal of environmental radioactivity* (101) p. 773-779
- Beks, J,P, Eisma, D and Der Plicht, J. 1998. A record of atmospheric 210Pb deposition in the Netherlands. *Science of the total environment* (222) p. 35-44
- Biester, H, Bindler,R, Martinez-Cortizas,M and Engstrom, D,R. 2007. Modeling the past atmospheric deposition of mercury using natural archives. *Environmental science and technology* (41) p. 4851-4860
- Bindler, R, Klarqvist, M, Klaminder, J and Förster, J. (2004). Dose within- bog spatial variability of mercury and lead constrain reconstructions of absolute deposition rates from single peat records? The example of store mosse, Sweden. *Global biogeochemical cycles* (18)
- Blume- Werry, G, Milbau, A, Teuber, L,M, Johansson, M, Dorrepaal, E. (2019) Dwelling in the deep- strongly increased root growth and rooting depth enhance plant interactions with thawing permafrost soil. *New phytologist* (223) p. 1328-1339
- Castro, D, Souto, M, Garcia-Rodeja, E, Pontevedra- Pombal, X and Fraga, M,I. 2014. Climate change records between the mid- and late Holocene in peat bog from Serra do Xistral (SW Europe) using plant macrofossils and peat humification analyses. *Palaeogeography Palaeoclimatology Palaeoecology* (420) 82-95
- Davies, L,J, Appleby, P, Jensen, B,J,L, Magnan, G, Mullan- Boudreau, G, Noernberg, T, Shannon,B, Shotyk, W, Van Bellen, S, Zaccane, C and Froese, D,G. 2018. High- resolution age modelling of peat bogs from northern Alberta, Canada, using pre- and post- bomb <sup>14</sup>C, <sup>210</sup>Pb and historical cryptotephra. *Quaternary Geochronology* (47) p. 138-162
- Drexler, J,Z, Alpers, C,N, Neymark, L,A, Paces, J,B, Taylor, H,E and Fuller, C,C. 2016. Amillennial-scale record of Pb and Hg contamination in peatlands of the Sacramento–San Joaquin Delta of California, USA. *Science of the total environment* (551-552) p. 738-751
- Dorrepaal, E, Toet,S, Van Logtestijn, R,S,P, Swart, E, Van de weg, M,J, Callaghan, T,V and Aerts,R. 2009. Carbon respiration from subsurface peat accelerated by climate warming in the subartic. *Nature* (460) p. 616
- Gong, S-Y, Li, H-C, Siringan, F,P, Zhao, M, Kang, S-C, Chou, C-Y. 2017. AMS Carbon- 14 dating of microbial carbonates in Holocene coral reefs, Western Luzon, Philippines. *Quaternary International* (447) p. 27-34
- Haesaerts, P, Borziac, I, Chekha, V,P, Chirica, V, Drozdov, N,I, Koulakovska, L, Orlova, L,A, Van der Plicht, J, Damblon, F. 2010. Charcoal and wood remains for radiocarbon dating upper Pleistocene loess sequences in Eastern Europe and Central Siberia. *Palaeogeography Palaeoclimatology Palaeoecology* (291) p. 106-127
- Hansson, S,V, Kaste, J,M, Chen, K and Bindler, R. (2014). Beryllium-7 as a natural tracer for short-term downwash in peat. *Biogeochemistry* (119) p. 329-339
- Hansson, S,V, Tolu. J and Bindler. R. (2015). Downwash of atmospherically deposited trace metals in peat and the influence of rainfall intensity: An experiment test. *Science of the total environment* p. 95-101

Johansson, M, Callahan, T,V, Bosiö, J, Åkerman, H,J, Jackowicz- Korczynski, M and Christensen, T,R. (2013). Rapid responses of permafrost and vegetation to experimentally increased snow cover in sub- arctic Sweden. *Environmental research letters* (8)

MacKenzie, A,B, Farmer, J,G, Sugden, C,L. (1997). Isotopic evidence of the relative retention and mobility of lead and radiocaesium in Scottish ombrotrophic peats. *The science of the total environment* (203) p. 115-127

MacKenzie, A,B, Hardie, S,M,L, Farmer, J,G, Eades, L,J, Pulford, I,D. 2010. Analytical and sampling constraints in  $^{210}\text{Pb}$  dating. *Science of the total environment* p. 1298-1304  
Malmer, N and Wallén, B. 1999. The dynamics of peat accumulation on bogs: mass balance of hummocks and hollows and its variation throughout a millennium. *Ecography* (22) p. 736-750

Marx, S,K, Kamber, B,S, McGowan, H,A, Zawadzki, A. 2009. Atmospheric pollutants in alpine peat bogs record a detailed chronology of industrial and agricultural development on the Australian continent. *Environmental pollution* (158) p. 1615-1628

Olid, C, Garcia-Orellana, J, Martínez- Cortizas, A, Masqué, P, Peiteado, E, and Sanchez-Cabeza, J,A. 2008 Role of surface vegetation in Pb-dating of peat cores. *Environmental science & technology* (42) p. 8858- 8864.

Olid, C, Garcia- Orellana, J, Martínez- Cortizas, A, Masqué, P, Peiteado- Varela, E, Sanchez- Cabeza, J-A. (2010). Multiple site study of recent atmospheric metal (Pb, Zn and Cu) deposition in the NW Iberian Peninsula using peat cores. *Science of the total environment* (408) p. 5540- 5549

Olid,C, Garcia- Orellana, J, Masqué, P, Martínez- Cortizas, A, Sanchez-Cabeza, J,A and Bindler, R. 2013. Improving the  $^{210}\text{Pb}$ - chronology of Pb deposition in peat cores from Chao de Lamoso (NW Spain). *Science of the total environment* (443) p. 597-607

Olid, C. personal communication

Olidfield, F, Richardson, N and Appleby, P.G. 1995. Radiometric dating ( $^{210}\text{Pb}$ ,  $^{137}\text{Cs}$ ,  $^{241}\text{Am}$ ) of recent ombrotrophic peat accumulation and evidence for changes in mass balance. *The Holocene* (5) p. 141-148

Paatero, J, Vaaramaa, K, Buyukay, M, Hatakka, J and Lehto, J. 2015. Deposition of atmospheric  $^{210}\text{Pb}$  and total beta activity in Finland. *Journal of radioanalytical and nuclear chemistry* (303) p. 2413-2420

Ralska- Jasiewiczowa, M, Madeyska, E and Mierzéńska, M. 2006. Vegetation changes in the montane grassland zone of the high bieszczady mountains southeast Poland during the last millennium- pollen records from deposits in hanging peat- bogs. *Veget hist archaeobot* (15) p. 391-401

Sanchez- Cabeza, J,A, Masqué, P, Ani- Ragolta, L. 1998.  $^{210}\text{Pb}$  and  $^{210}\text{Po}$  analysis in sediments and soils by microwave acid digestion. *Journal of radioanalytical and nuclear chemistry* (227) p. 19-22.

Taylor, A, Blake, W,H, Couldrick, L, Keith- Roach, M,J. 2011. Sorption behaviour of beryllium- 7 and implications for its use as a sediment tracer. *Geoderma* p. 16-23  
UNSCEAR. 2000. Sources and effects of ionizing radiation. *Journal of radiological protection* (21)

Vile, M,A, Wieder, R,K, and Novák, M. 1999. Mobility of Pb in sphagnum- derived peat. *Biogeochemistry* (45) p. 35-52.

Wang, p, Mommer, L, Van Ruijven, J, Betendse, F, Maximov, T, C and Heijmans, M, M,P,D. 2016. Seasonal changes and vertical distribution of root standing biomass of graminoids and shrubs at a Siberian tundra site. *Plant soil* (407) p. 55-65

Zalewska, T, Przygodzki, P, Suplińska, M and Saniewski, M. 2020. Geochronology of the southern Baltic Sea sediments derived from  $^{210}\text{Pb}$  dating. *Quaternary Geochronology* (56)